J Biomol NMR (2012) 54:33–42
DOI 10.1007/s10858-012-9647-0

ARTICLE

High resolution methyl selective ^{13}C-NMR of proteins in solution and solid state

Garima Jaipuria · Nitin Prakash Lobo · Divya Shet · Hanudatta S. Atreya

Received: 2 May 2012 / Accepted: 19 June 2012 / Published online: 11 July 2012

Abstract New ^{13}C-detected NMR experiments have been devised for molecules in solution and solid state, which provide chemical shift correlations of methyl groups with high resolution, selectivity and sensitivity. The experiments achieve selective methyl detection by exploiting the one bond J-coupling between the ^{13}C-methyl nucleus and its directly attached ^{13}C spin in a molecule. In proteins such correlations edit the ^{13}C-resonances of different methyl containing residues into distinct spectral regions yielding a high resolution spectrum. This has a range of applications as exemplified for different systems such as large proteins, intrinsically disordered polypeptides and proteins with a paramagnetic centre.

Keywords Methyl groups · Methyl COSY · Methyl selective NMR · ^{13}C direct detection · Solid state NMR · Paramagnetic proteins

Electronic supplementary material The online version of this article (doi:10.1007/s10858-012-9647-0) contains supplementary material, which is available to authorized users.

G. Jaipuria · N. P. Lobo · D. Shet · H. S. Atreya (✉)
NMR Research Centre, Indian Institute of Science, Bangalore 560012, India
e-mail: hsatreya@sif.iisc.ernet.in

G. Jaipuria · H. S. Atreya
Solid State and Structural Chemistry Unit, Indian Institute of Science, Bangalore 560012, India

N. P. Lobo
Department of Physics, Indian Institute of Science, Bangalore 560012, India

Introduction

The hydrophobic core of proteins and interfaces in protein–protein complexes are enriched with methyl group containing amino acids which provide crucial long range distance information for structure determination (Metzler et al. 1996; Gardner et al. 1997; Zheng et al. 2003; Zech et al. 2004). Further, rapid rotation about their threefold axis together with three chemically equivalent protons results in their signals with high intensity (Nicholson et al. 1992; Gagne et al. 1998; Choy and Kay 2003). This has led to the development of methods that exploit these characteristics for structural and dynamic studies in proteins (Werbelow and Marshall 1973; Gardner et al. 1996, 1997; Rosen et al. 1996; Zwahlen et al. 1998; Tugarinov et al. 2003; Gross et al. 2003; Tugarinov et al. 2004; Tugarinov and Kay 2004; Tugarinov et al. 2005). However, among methyl groups there is significant overlap of chemical shifts (Fig. 1). Typically, their ^{13}C and ^{1}H shifts occur in the range of 10–30 and 0–1.5 ppm, respectively (Atreya and Chary 2001). This overlap can be removed in two ways. First, by correlating the chemical shift of a methyl carbon with that of its directly attached neighboring carbon nucleus, which results in distinct ^{13}C shifts for the different methyl group containing amino acid types (Barnwal et al. 2008; Jaipuria et al. 2010). Second, employing ^{13}C detection provides superior resolution (Kovacs et al. 2005; Bermel et al. 2006) (Fig. 1). Combining these two principles, we present a new experiment called 2D ^{13}C-Methyl COSY which affords a significant separation of methyl groups as illustrated in Fig. 1.

An additional feature is the selective detection of ^{13}C-resonances of methyl groups ($^{13}C^{met}$). This is achieved by exploiting the fact that only $^{13}C^{met}$ (located at the terminal end of the amino acid chain) has a single one-bond J-coupled partner, $^{13}C^{neigh}$ (i.e., its directly attached

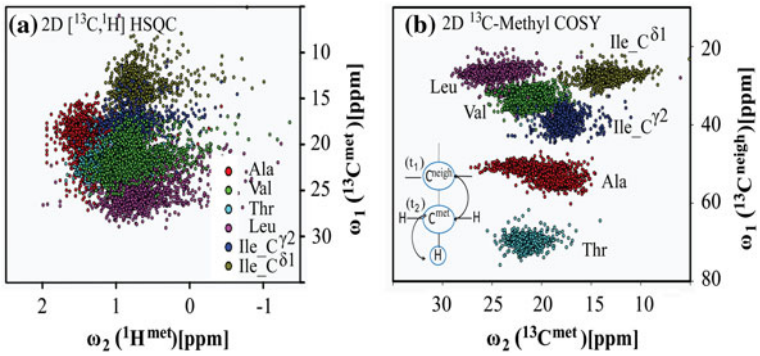

Fig. 1 **a** Simulated spectrum depicting overlap of methyl resonances in a conventional 2D [^{13}C, ^{1}H] HSQC. **b** Simulated 2D ^{13}C-Methyl COSY spectrum illustrating the resolution of overlaps. The simulations have been carried out using data from 186 proteins from the BioMagResBank (BMRB; http://www.bmrb.wisc.edu) database

neighboring ^{13}C spin). When a delay of $1/2J_{CC}$ ($J_{CC} \sim 35$ Hz) is used, $^{13}C^{met}$ has a single active coupled spin whereas other ^{13}C nuclei are dephased with respect to two or three ^{13}C-spins (Jaipuria et al. 2010; Barnwal et al. 2008). This simplifies the spectrum in the methyl region (0–30 ppm in ^{13}C) by filtering out signals from overlapping non-methyl containing amino acids such as Lys and Arg (Atreya and Chary 2001). Thus, the only correlations observed in the methyl region are $^{13}C^{neigh}$–$^{13}C^{met}$. Based on this principle, we present novel ^{13}C-methyl correlation experiments for molecules in solution and solid state which can be acquired rapidly and provide selective methyl correlations with high resolution. The 2D ^{13}C-Methyl COSY can be incorporated as a resolving plane in a 3D or 4D experiment wherein the additional dimensions can be utilized to provide intra-amino acid or long-range correlations. For instance, in the solid state a ^{13}C-Dipolar assisted rotational resonance (DARR) module (Takegoshi et al. 2001, 2003) can be added to the 2D experiment to obtain correlation to ^{13}C-spins dipolar coupled to the methyl carbons. Similarly in the solution state, a ^{13}C-TOCSY module (Cavanagh et al. 2007) can be added resulting in 3D ^{13}C-TOCSY-Methyl COSY. The experiments presented here afford a range of applications in resonance assignment and structure determination of proteins as exemplified for different systems such as large proteins (Maltose binding protein; 42 kDa), intrinsically disordered polypeptides [LIGFBP-2: the 12 kDa central flexible domain of insulin-like growth factor binding protein-2 (Swain et al. 2010; Chandra et al. 2012)] and proteins with a paramagnetic centre (Cu(II)-ubiquitin). In the case of paramagnetic Cu-bound ubiquitin accurate measurement of methyl ^{1}H transverse relaxation enhancements provided information on the position of the metal ion with respect to the 3D structure of the protein.

The different 2D and 3D experiments implemented in solution and solid state are summarized in Table 1 and set of radio frequency (r.f.) pulse schemes are shown in Fig. 2. The methyl selection scheme is illustrated in Fig. 2a. For non-deuterated proteins the experiments start with the transfer of polarization from $^{1}H^{met}$ to $^{13}C^{met}$ (using INEPT in solution state and CP in solids) followed by transfer of polarization from $^{13}C^{met}$ to its directly attached ^{13}C spins (denoted as $^{13}C^{neigh}$) (Jaipuria et al. 2010). This is accomplished using one-bond ^{13}C J-coupling ($\sim$35 Hz). The $^{13}C^{neigh}$ nucleus is frequency labeled (during t_1) and the polarization is transferred back to $^{13}C^{met}$ for detection (during t_2). The delay periods, $\tau2 + \tau3 + \tau4$ and $2 \times \tau5$ (Fig. 2a) for out and back $^{13}C^{met} \rightarrow {}^{13}C^{neigh}$ magnetization transfer, respectively, is set to $1/2J_{CC} \sim 14$ ms to achieve maximum polarization transfer. During this delay period the signals relax primarily due to T_2 relaxation of $^{13}C^{met}$ which is given as $\exp(-4\tau_4/T_2)$. Assuming a T_2 of 100 ms for proteins with a rotational correlation time of 7–8 ns (Nicholson et al. 1992) this yields a loss of $\sim$25–30 % in signal intensity. The delay can be set to values smaller than 14 ms for systems with shorter $T_{2(^{13}C-met)}$. However this results in the incomplete transfer of magnetization from $^{13}C^{met}$ to $^{13}C^{neigh}$ and hence during t_1 chemical shift

Table 1 Summary of 2D/3D Methyl-COSY experiments

Solution/solid state	Experiment name	Chemical shifts correlated	R.f. pulse scheme
Solution	2D ^{13}C-Methyl COSY	ω_1 ($^{13}C^{neigh}$) ω_2 ($^{13}C^{met}$)	Fig. 2a
Solution	3D ^{13}C-TOCSY-Methyl COSY	ω_1 (^{13}C), ω_2 ($^{13}C^{neigh}$), ω_3 ($^{13}C^{met}$)	Fig. 2b, c
Solid	2D ^{13}C-Methyl COSY	ω_1 ($^{13}C^{neigh}$) ω_2 ($^{13}C^{met}$)	Fig. 2d
Solid	2D ^{13}C-DARR-Methyl COSY	ω_1 ($^{13}C^{neigh}$) ω_2 ($^{13}C/^{13}C^{met}$)	Fig. 2e

evolution period both $^{13}C^{met}$ and $^{13}C^{neigh}$ are frequency labelled. The $^{13}C^{met}$ magnetization is subsequently detected during t_2 resulting in the appearance of diagonal peaks [at $\omega_1(^{13}C^{met})$, $\omega_2(^{13}C^{met})$] which can potentially overlap with the cross peaks of leucine which has similar $^{13}C^{met}$, $^{13}C^{neigh}$ shifts and hence lies close to the diagonal. In all the applications presented here the delay for $^{13}C^{met} \rightarrow {}^{13}C^{neigh}$ transfer was set to $\sim$14.0 ms in solution state (Fig. 2a–c) and 11 ms for solid state (Fig. 2d, e). In the case of per-deuterated proteins, the polarization starts directly from $^{13}C^{met}$ instead of ^{1}H as shown in Fig. 2c. Additionally, ^{1}H decoupling is replaced by ^{2}H decoupling. The IPAP mode of acquisition (Ottiger et al. 1998) is applied for solution state experiments to improve sensitivity and resolution (Bermel et al. 2008). The in-phase spectrum is acquired using the r.f. sequence shown in Fig. 2a–c and for acquiring the anti-phase component, the second ^{13}C–^{13}C magnetization transfer part (required for the return of magnetization from $^{13}C^{neigh}$ to $^{13}C^{met}$; shown in box in Fig. 2a–c) is omitted. This results in the detection of the anti-phase magnetization: $^{13}C_x^{met}{}^{13}C_z^{neigh}$. The anti-phase spectra is then linearly combined with the in-phase spectrum in a manner similar to that used routinely for processing ^{13}C-detected spectra in the solution state (Bermel et al. 2006). Due to the differences in delay periods used for acquiring the two components, the in-phase and anti-phase spectra have slightly different intensities as illustrated in Figure S1 (Supporting Information). However due to the long $^{13}C^{met}$ transverse relaxation times, no significant differences were observed and on an average the ratio of the two (anti-phase/in-phase) components was $\sim$1.1 across the three proteins studied. Hence, no relative scaling factors were used and the two components were linearly combined with 1:1 ratio with minimal resulting residual signals (Figure S1). The IPAP mode of acquisition is not used in the solid state due to the observed broad lines limited by the rapid transverse relaxation rates. The spectra are acquired with an acquisition time (t_{max}) of 72 ms in the solution state and 20 ms in the solid state yielding linewidths of $\sim$17 and $\sim$100 Hz, respectively, in the direct dimension. The resolution in the indirect dimension is governed primarily by the transverse relaxation of ^{13}C spin attached to ^{13}C-methyl and spectra are typically acquired with t_{max} of 9 and 5 ms in solution and solid state, respectively.

Notably, the method used here for spin state selection is different and simplified compared to two approaches proposed earlier for narrowing of ^{13}C-detected methyl signals in solution state (Jordan et al. 2006; Bermel et al. 2007). In one approach (Jordan et al. 2006) maximum entropy reconstruction-deconvolution was used in a post-acquisition manner to remove the effect of ^{13}C–^{13}C coupling and to obtain narrower lines. However, such a method is computationally intensive and hence the authors recommended analyzing in parallel both the conventionally acquired spectrum (without ^{13}C–^{13}C decoupling) and the spectrum with ^{13}C–^{13}C couplings deconvoluted using the maximum entropy method. In the second approach (Bermel et al. 2007), effect of ^{13}C–^{13}C coupling for methyl groups (of alanine) was removed using the S^3E approach, the building block of which consisted of selective r.f. pulses pulses on $^{13}C^{met}$ and $^{13}C^{\alpha}$ and a delay period of $1/4J_{CC}$ (7.2 ms) involving the coupling of $^{13}C^{met}$ to $^{13}C^{\alpha}$. Two spectra were acquired with each containing both the in-phase and anti-phase components with different relative signs followed by their appropriate linear combination. In general, this approach cannot be applied to the method proposed here since the $^{13}C^{neigh}$ spans the entire ^{13}C range (0–80 ppm) and are not separated from the $^{13}C^{met}$ region (e.g., C^{neigh} of Leucine is as close as $\sim$2 ppm to C^{met} of Leucine). The alternative method proposed here is thus simplified compared to these approaches and does not require any selective r.f. pulses or/and special post-acquisition processing methods.

Figure 3 shows the 2D ^{13}C-Methyl COSY spectra acquired for MBP and Ubiquitin (acquisition parameters are given in Table S1 of Supporting Information) processed with NMRPipe (Delaglio et al. 1995) and analyzed using XEASY (Bartels et al. 1995). The preparation of the samples has been described previously (Chandra et al. 2012). All NMR samples used contained $\sim$1.0 mM of the protein in 95 % H_2O/5 % $^{2}H_2O$. The experiments are sensitive in nature as evident from the distribution of signal-to-noise (S/N) ranging typically from $\sim$10–30 for cross peaks in spectra acquired for 1 mM sample of three proteins: Maltose binding protein (42 kDa), L-IGFBP2 (12 kDa) and Ubiquitin (Figure S2 of Supporting Information). Each of 2D spectra was acquired with measurement time ranging from 20 min to 2 h (acquisition parameters are given in Table S1 of Supporting Information).

The experiment is particularly useful for assignment of unfolded or intrinsically unstructured polypeptides which lack good dispersion in $^{1}H/^{13}C$ shifts. Even though the ^{13}C signals from a given methyl amino acid type occur in the same region of the spectrum in 2D ^{13}C-Methyl COSY, they are well resolved due to the inherent dispersion of $^{13}C^{met}$–$^{13}C^{neigh}$ correlations together with sharp lines observed in contrast to line broadening in ^{1}H-based detection. This is evident in the spectrum acquired for structurally disordered protein, L-IGFBP2 (12 kDa) (Swain et al. 2010; Chandra et al. 2012). Figure 4a shows a region of the conventionally acquired 2D ^{13}C–^{1}H HSQC spectrum with significant overlap of methyl chemical shifts due to which many of the resonances could not be assigned.

However, they are resolved in 2D ^{13}C-Methyl COSY (Fig. 4b). The expanded regions of the spectrum show that all the signals of Ala, Val and Thr could be resolved. The assignment of methyl signals sequence specifically can be obtained using 3D ^{13}C-TOCSY-Methyl COSY (Fig. 2b, c) which correlates the chemical shifts of methyl ^{13}C with their respective backbone $^{13}C^{\alpha}$ and $^{13}C^{\beta}$ resonances. Figure 4c illustrates the 3D ^{13}C-TOCSY-Methyl COSY spectrum of L-IGFBP2.

In the solid state, the 2D ^{13}C-Methyl COSY (Fig. 2d, e) provides a method to selectively detect resonances from methyl group containing amino acids. The transfer of magnetization between the neighbouring carbon nuclei is accomplished using J-coupling (Andronesi et al. 2005; Elena et al. 2005; Chen et al. 2007a, b; Tian et al. 2009; Zhong et al. 2007) at high spinning speeds instead of the conventional dipolar based transfer. This is illustrated in Fig. 5a, which shows a 1D CP-MAS spectrum of a mixture of ^{13}C,^{15}N labeled Valine and Lysine acquired at a spinning frequency of 25 kHz. Figure 5b shows the 1D projection of the spectrum acquired on the same sample using the r.f. pulse scheme shown in Fig. 2e. Thus, in a mixture of lysine and valine only correlations from valine are observed (Fig. 5b).

Editing of methyl groups into distinct spectral regions is illustrated in Fig. 6 which shows the spectra acquired for a mixture of three amino acids: Val, Ala and Thr. In the conventionally acquired 2D ^{13}C–^{13}C correlation spectrum the resonances of Ala ($^{13}C^{\beta}$) and Thr ($^{13}C\gamma^{2}$) overlap (Fig. 6a). They are well resolved in 2D Methyl-COSY (Fig. 6b) due to the distinct chemical shifts of Ala ($^{13}C^{\alpha}$) and Thr ($^{13}C^{\beta}$), respectively. Figure 6d exemplifies the application of 2D ^{13}C-DARR-Methyl-COSY wherein the set of cross peaks of Ala ($^{13}C^{\beta}$) and Thr ($^{13}C\gamma^{2}$) which would have overlapped in a conventionally acquired 2D DARR (Fig. 6c) are resolved completely (Fig. 6d). In the case of proteins, the 2D ^{13}C-Methyl-COSY can be acquired with high sensitivity and is devoid of artifacts as illustrated in Figure S3 (Supporting Information). Figure 2e shows the r.f. pulse scheme of ^{13}C-DARR-Methyl-COSY, which utilizes the 2D ^{13}C-Methyl COSY to resolve intra-amino acid long-range correlations.

One application of 2D Methyl-COSY in the solution state is illustrated for the measurement of methyl ^{1}H paramagnetic relaxation enhancements (PREs). In proteins with a paramagnetic metal centre PREs provide valuable structural constraints for structure calculations (Bertini et al. 2002; Clore and Iwahara 2009; Iwahara et al. 2007). In particular, they provide long range distance information (10–30 Å) which is inaccessible in the conventional Nuclear Overhauser Effect (NOE) based methods. The ^{1}H PREs of ^{15}N or ^{13}C bound protons are typically measured using a 2D [^{15}N–^{1}H] HSQC or a 2D [^{13}C–^{1}H] HSQC, respectively (Iwahara et al. 2007). However, in the case of broadening and/or overlap of ^{1}H resonances, the PREs cannot be measured accurately. In such cases, 2D ^{13}C-Methyl COSY which provides good resolution can be used. This was useful for determining the position of the metal ion in Cu(II)-ubiquitin (Fig. 7), implicated in neurogenerative disorders (Milardi et al. 2007; Arnesano et al. 2009; Arnesano 2010). Copper (Cu(II)) has been reported to bind near residues Met-1 and His-68 of ubiquitin. However a 3D structure of Cu-bound Ubiquitin has not been determined. The 2D ^{13}C-Methyl COSY was used for measuring ^{1}H PREs in Cu(II)-ubiquitin due to overlap of ^{1}H-methyl shifts of amino acid residues arising from line broadening ($C^{\gamma 2}$ V70-$C^{\gamma 2}$ T66; $C^{\gamma 2}$ T9-$C^{\gamma 2}$ T22) in the 2D [^{13}C,^{1}H] HSQC.

The ^{1}H transverse paramagnetic relaxation enhancements (PREs) on Cu-ubiquitin were measured using a modified version of 2D ^{13}C Methyl-COSY described below (Figure S4 of Supporting Information). The PREs (Γ) were calculated

Fig. 2 a–e R.f. pulse schemes of ^{13}C-detected methyl selective correlation experiments for solution and solid state. *Thin* and *thick vertical bars* indicate rectangular 90° and 180° pulses, respectively, and the RF phases are indicated above the pulses. Where no r.f. phase is marked, the pulse is applied along *x*. High power 90° pulse lengths are: 15.0 μs for ^{1}H and 10.5 μs for ^{13}C in the solution state and 2.5 μs for ^{1}H, 5 μs for ^{13}C in the solid state experiments. The ^{13}C r.f. carrier is placed at 40 ppm and the ^{1}H carrier position is set to 4.7 ppm throughout the duration of the experiment. **a** 2D ^{13}C-Methyl COSY (solution state). WALTZ-16 is employed to decouple ^{13}C from ^{1}H. Spectral width of 80 ppm is chosen for both the ^{13}C dimensions. The delays are: $\tau_1 = 2$ ms, $\tau_2 = 0.8$ ms, $\tau_3 = 4.95$ ms, $\tau_4 = \tau_5 = 7.0$ ms. Phase cycling: $\Phi_1 = \Phi_2 = x, -x, -x, x$; Φ (receiver) $= x, -x, -x, x$. Quadrature detection in t_1 ($^{13}C^{Neigh}$) is carried out in States manner (i.e., $\Phi_2 = x, y$). For the AP (antiphase version), the part of the sequence shown in box is omitted. That is, acquisition starts immediately after the 90° pulse following t_1. **b** 3D ^{13}C-TOCSY-Methyl COSY. The delays are: $\tau_1 = 2$ ms, $\tau_2 = 0.8$ ms, $\tau_3 = 7$ ms. Phase cycling: $\Phi_1 = x, -x, -x, x$, $\Phi_2 = x$; Φ(receiver) $= x, -x, -x, x$. Quadrature detection in t_1 and t_2 is carried out in States manner. Phases are varied as $\Phi_2 = x, y$, $\Phi_3 = y, x$, $\Phi_4 = x, y$. All other acquisition parameters are same as the 2D ^{13}C-Methyl COSY shown in **a** including the IPAP mode of detection. **c** R.f. pulse scheme of 3D ^{13}C-TOCSY-Methyl COSY (starting from direct ^{13}C-polarization) for deuterated proteins in solution state. The delays are: $\tau_1 = 2$ ms, $\tau_2 = 0.8$ ms, $\tau_3 = 7.0$ ms. Phase cycling: $\Phi_1 = \Phi$(receiver) $= x, -x, -x, x, y, -y, -y, y$. Spectral width of 80 ppm has been chosen in all the three dimensions. Quadrature detection in t_1 and t_2 is carried out in States manner. Phases are varied as $\Phi_2 = x, y$, $\Phi_3 = y, x$. **d** R.f. pulse scheme of 2D ^{13}C-Methyl COSY (Solids). Ramped CP (Metz et al. 1994) is used for transfer of polarisation from ^{1}H and TPPM (Bennett et al. 1995) is employed to decouple ^{1}H (r.f. field strength = 100 kHz). The delays are: $\tau_2 = 6.0$ ms. Phase cycling: $\Phi_1 = y, -y$; $\Phi_2 = x, x, -x, -x$; $\Phi_3 = x, -x$; Φ_4(receiver) $= x, -x, -x, x$. Quadrature detection in t_1($^{13}C^{Neigh}$) is carried out in States manner (i.e., $\Phi_3 = x, y$). **e** R.f. pulse scheme of 2D ^{13}C-DARR-Methyl COSY in solid state. DARR is applied at MAS spinning rate of 11,111 Hz. The delays are: $\tau_2 = 6.0$ ms. Phase cycling: $\Phi_1 = y, -y$; $\Phi_2 = x, x, -x, -x$; $\Phi_3 = x, -x$; Φ_4(receiver) $= x, -x, -x, x$. Quadrature detection of t_1($^{13}C^{Neigh}$) is carried out in States manner (i.e., $\Phi_3 = x, y$). All other acquisition parameters are the same as those in 2D ^{13}C-Methyl COSY (Solids) experiment **d**

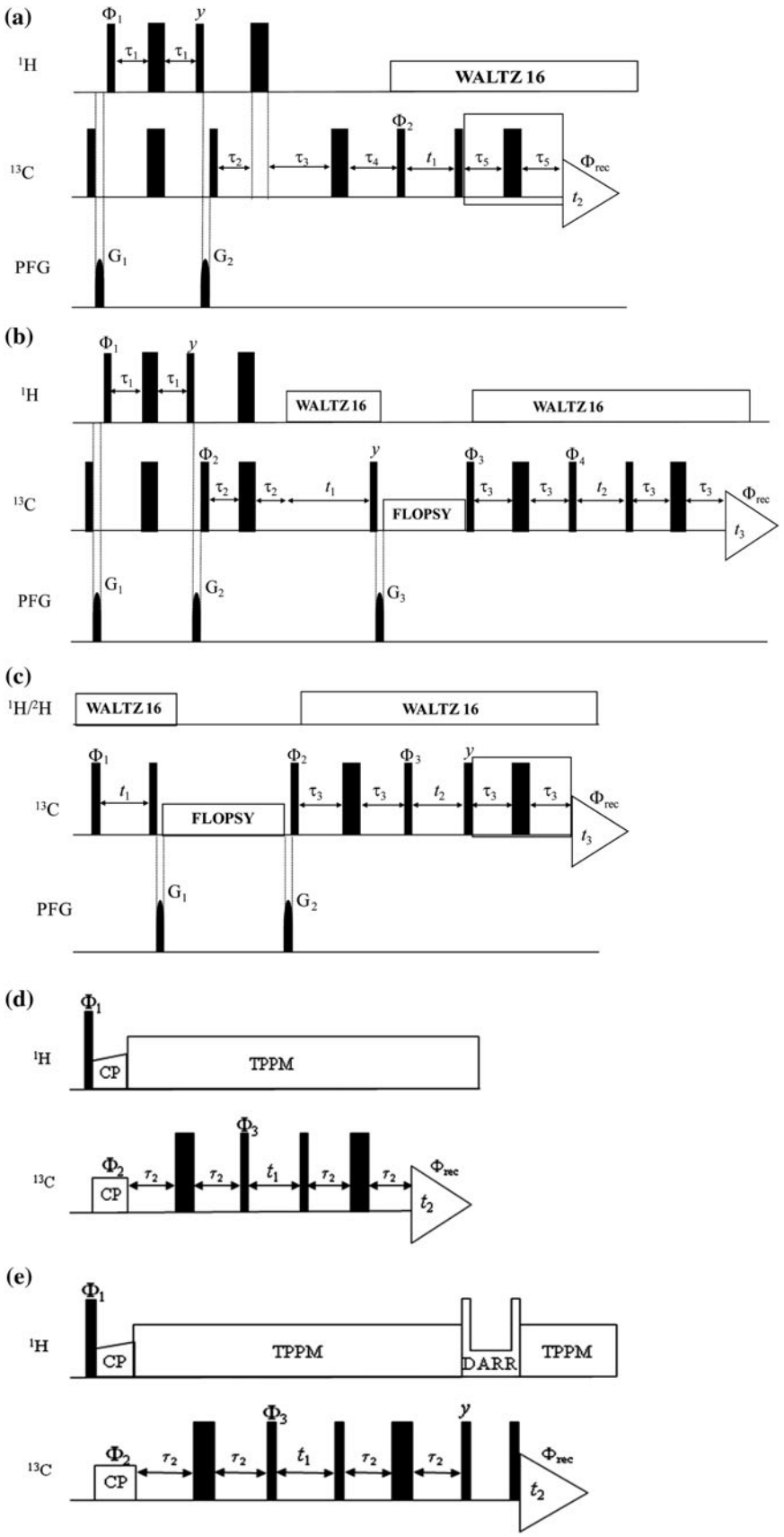
(a)
Φ1
y
τ1
τ1
1H
WALTZ 16
Φ2
13C
τ2
τ3
τ4
t1
τ5
τ5
Φrec
t2
PFG
G1
G2
(b)
Φ1
y
τ1
τ1
1H
WALTZ 16
WALTZ 16
Φ2
y
Φ3
Φ4
13C
τ2
τ2
t1
FLOPSY
τ3
τ3
t2
τ3
τ3
Φrec
t3
PFG
G1
G2
G3
(c)
1H/2H
WALTZ 16
WALTZ 16
Φ1
Φ2
Φ3
y
13C
t1
FLOPSY
τ3
τ3
t2
τ3
τ3
Φrec
t3
PFG
G1
G2
(d)
Φ1
1H
CP
TPPM
Φ3
Φ2
13C
CP
τ2
τ2
t1
τ2
τ2
Φrec
t2
(e)
Φ1
1H
CP
TPPM
DARR
TPPM
Φ3
y
Φ2
13C
CP
τ2
τ2
t1
τ2
τ2
Φrec
t2

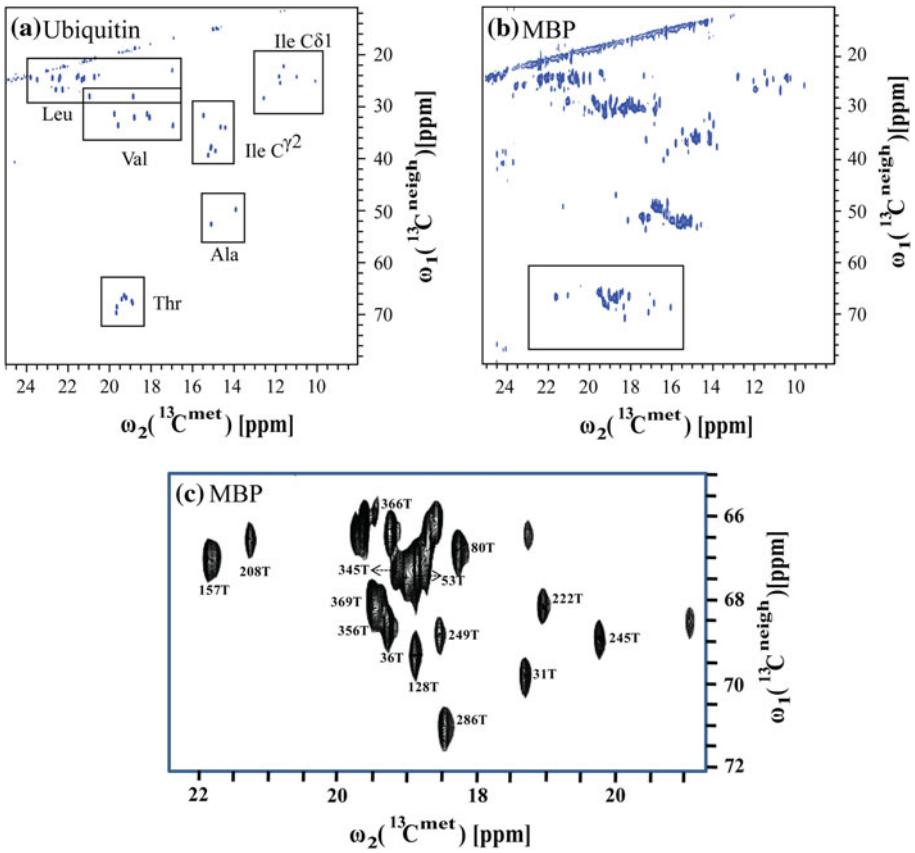

Fig. 3 2D ^{13}C methyl COSY spectra acquired for: **a** Ubiquitin **b** MBP in solution. In **c** the expanded Threonine region of MBP is shown which gets resolved due to inherent resolution imparted by their C^{met}, C^{neigh} chemical shifts which are exploited in the ^{13}C methyl COSY experiment. The spectra were acquired at 25 °C on a 700 MHz NMR spectrometer equipped with a cryogenic probe

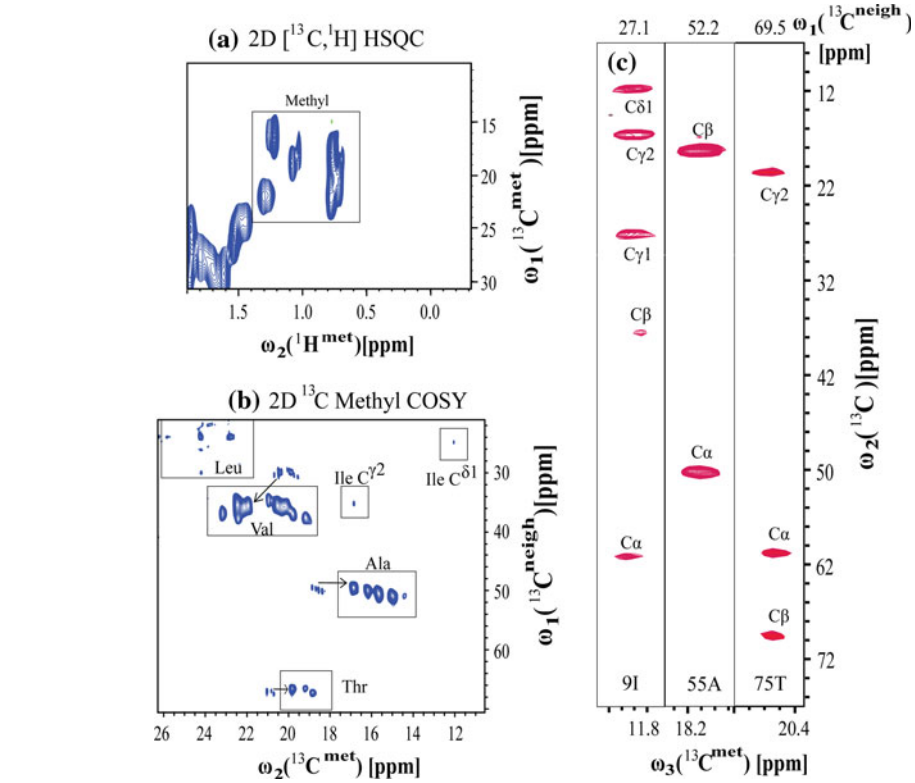

Fig. 4 **a** 2D ^{13}C–^{1}H HSQC, **b** 2D ^{13}C-Methyl COSY and **c** representative 2D [$\omega_2(^{13}C)$–$\omega_3(^{13}C)$] strips from ^{13}C-TOCSY-Methyl COSY spectrum of structurally disordered L-IGFBP2 in solution. The *insets* in **b** show enlarged Val, Ala and Thr regions. Please note that the protein has only one Ile which has not been enlarged but marked in the Methyl-COSY spectrum. In **c** the residues assigned are indicated at the bottom in each strip. The spectra were acquired at 25 °C on a Bruker Avance 700 NMR spectrometer equipped with a cryogenic probe

from the peak intensities (peak volumes) based on the approach described for measurement of PREs from a regular 2D [^{15}N–^{1}H]/[^{13}C–^{1}H] HSQC (Iwahara et al. 2007) as follows:

$$\Gamma_2 = \frac{1}{15}\left(\frac{\mu_0}{4\pi}\right)^2 \gamma_I^2 g^2 \mu_B^2 S(S+1) r^{-6} \left\{ 4\tau_c + \frac{3\tau_c}{1+(\omega_H \tau_c)^2} \right\} \quad (1)$$

The distances of the metal ion ('r') from the protein were then calculated using:

$$\Gamma_2 = R_{2,para} - R_{2,dia} = \frac{1}{T_b - T_a} \ln \left\{ \frac{I_{dia}(T_b) I_{para}(T_a)}{I_{dia}(T_a) I_{para}(T_b)} \right\} \quad (2)$$

Where, I_{dia} (T_a/T_b) and I_{para} (T_a/T_b) are the peak volumes of peaks in spectra acquired for apo and Cu-bound protein, respectively, at $T_a = 0$ ms (i.e., d25 = 0 in Figure S4) and $T_b = 20$ ms (i.e., d25 = 5 ms in Figure S4). And, $\mu_0/4\pi = 10^{-7}$ Tm/A $\gamma_I = 2.67 \times 10^8$ Ts^{-1}, $g = 2.002$, $\mu_B = 9.274 \times 10^{-24}$ JT^{-1}, $S = 0.5$, $\tau_c = 4 \times 10^{-9}$ s, $\omega_H = 2 \times 3.14 \times 700 \times 10^6$ Hz.

The ^{1}H PREs calculated above were used for structure calculations (Fig. 7). The position of the metal ion was calculated starting from a high-resolution structure of Ubiquitin taken from the protein data bank (PDB code: 1UBQ). A total of 40 ^{1}H (methyl) and 51 $^{1}H^{N}$ upper limit constraints were used for the calculation. The list of distances calculated from the observed PREs is given in Table S2 of Supporting Information. Calculations were performed using CYANA v 3.93. The ubiquitin structure was regularized and torsion angles of the protein were fixed based on the observation that the protein does not undergo a conformational change upon binding copper (Milardi et al. 2007; Arnesano et al. 2009; Arnesano 2010). The distances of the atoms from the metal ion (d_i) as calculated from the observed PREs (Eqns. 1 and 2 above) were used as restraints with $d_i \pm 5$ Å as the upper and lower bounds, respectively. Since the structure calculations involve a fixed protein structure, only a total of 10 structures were calculated and 5 out of them with the lowest residual target function were chosen. The position of the metal ion obtained was compared with the putative site proposed recently (Milardi et al. 2007; Arnesano et al. 2009; Arnesano 2010). The r.m.s.d. of the position of the metal ion among the five structures was 0.54 Å. The accuracy of methyl ^{1}H PREs was verified by calculating two structures: one with distances calculated from NH and methyl ^{1}H PREs obtained from a regular 2D [^{15}N–^{1}H] HSQC and 2D [^{13}C–^{1}H] HSQC, respectively, and a second one as calculated above using the NH and methyl ^{1}H PREs obtained from 2D ^{13}C-Methyl COSY. The resulting r.m.s.d. was 1.3 Å thereby validating the methyl PREs obtained using 2D ^{13}C-Methyl COSY.

Conclusions

In summary, we have developed ^{13}C-detected NMR experiments which provide chemical shift correlations of methyl groups with high resolution, selectivity and sensitivity. They are based on correlation of ^{13}C-methyl chemical shifts with the directly attached ^{13}C spin which separates the methyl group containing amino acids into distinct spectral regions. The experiments have an inbuilt filter to selectively detect ^{13}C signals from the methyl groups of any molecule, which is achieved by exploiting the fact that the $^{13}C^{met}$ of the methyl group located at the terminal end of the amino acid chain has only a single one-bond J-coupling to its directly attached ^{13}C spin. This simplifies the spectrum by filtering out signals from overlapping non-methyl groups. The experiments have a range of applications and can be used a building block in three and higher dimensional experiments. For rapid

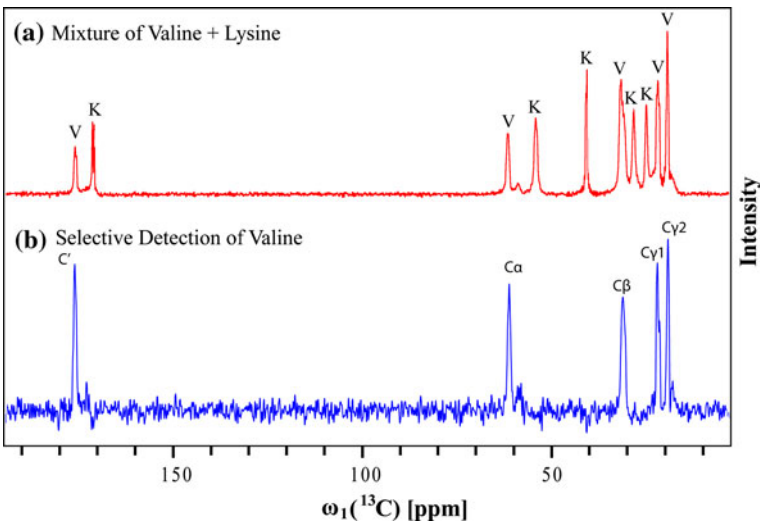

Fig. 5 **a** 1D CP-MAS spectrum of a mixture of 15 mg of ^{13}C,^{15}N labeled Valine and Lysine acquired at a spinning frequency of 25 kHz. **b** The ^{13}C resonances of valine (indicated) are selectively observed using the methyl correlation experiment (Fig. 2e). The spectra were acquired at 25 °C on a Bruker Avance 500 MHz NMR solid state spectrometer. The temperature was calibrated with a KBr sample using the method of Thruber and Tycko (2009)

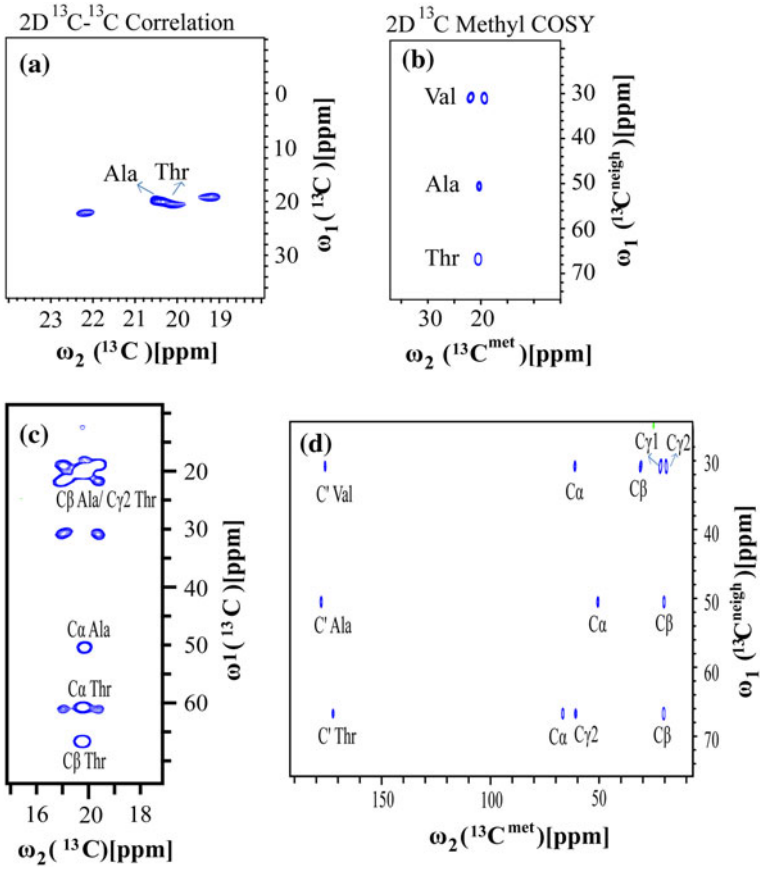

Fig. 6 **a** Conventional 2D ^{13}C–^{13}C Correlation and **b** 2D ^{13}C Methyl COSY spectrum of a mixture of ^{13}C labeled Val, Ala and Thr acquired in the solid state. **c** Conventional 2D ^{13}C–^{13}C DARR spectrum showing the overlap of Ala/Thr peaks. **d** Resolution of the overlap shown in **c** using 2D ^{13}C DARR Methyl-COSY acquired using r.f scheme shown in Fig. 2e

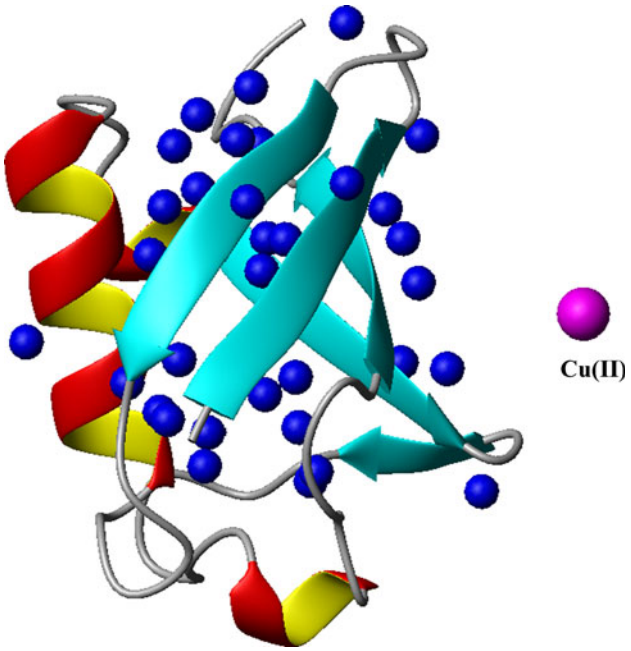

Fig. 7 3D Structure of Cu(II)-bound Ubiquitin. The position of the metal ion has been calculated using CYANA using 51 HN and 40 methyl ^{1}H PRE constraints with 1UBQ as the starting structure. The methyl groups which were used for measuring the PREs are indicated as blue spheres (tabulated in Table S2 of supporting information)

detection, new methods for rapid data collection especially those developed for methyl groups can be applied (Amero et al. 2009). This will provide new avenues for resonance assignment and structure determination of proteins in the solution and solid state.

Acknowledgments The facilities provided by NMR Research Centre at IISc supported by Department of Science and Technology (DST), India is gratefully acknowledged. HSA acknowledges support from Indo-Australia biotechnology fund awarded by the Department of Biotechnology (DBT). GJ acknowledges fellowship from Council of Scientific and Industrial Research (CSIR). The authors are sincerely thankful to Dr. Peter Güntert for useful discussions on structure calculation of Cu(II)-ubiquitin using CYANA. We thank Dr. John Cort, Pacific Northwest National Laboratory, for providing the Ubiquitin plasmid.

References

Amero C, Schanda P, Durá MA, Ayala I, Marion D, Franzetti B, Brutscher B, J Boisbouvier (2009) Fast two-dimensional NMR spectroscopy of high molecular weight protein assemblies. J Am Chem Soc 131:3448–3449

Andronesi OC, Becker S, Seidel K, Heise H, Young HS, Baldus M (2005) Determination of membrane protein structure and dynamics by magic-angle-spinning solid-state NMR spectroscopy. J Am Chem Soc 127:12965–12974

Arnesano F (2010) The role of copper ion and the ubiquitin system in neurodegenerative disorders. Ideas in chemistry and molecular sciences. Wiley, New York, pp 1–30

Arnesano F, Scintilla S, Calò V, Bonfrate E, Ingrosso C, Losacco M, Pellegrino T, Rizzarelli E, Natile G (2009) Copper-triggered aggregation of Ubiquitin. PLoS One 4:e7052

Atreya HS, Chary KVR (2001) Selective 'unlabeling' of amino acids in fractionally C-13 labeled proteins: an approach for stereospecific NMR assignments of CH_3 groups in Val and Leu residues. J Biomol NMR 19:267–272

Barnwal RP, Atreya HS, Chary KVR (2008) Chemical shift based editing of CH_3 groups in fractionally C-13-labelled proteins using GFT (3,2)D CT-HCCH-COSY: stereospecific assignments of CH_3 groups of Val and Leu residues. J Biomol NMR 42: 149–154

Bartels C, Xia TH, Billeter M, Güntert P, Wüthrich K (1995) The program xeasy for computer-supported NMR spectral-analysis of biological macromolecules. J Biomol NMR 6:1–10

Bennett AE, Rienstra CM, Auger M, Lakshmi KV, Griffin RG (1995) Heteronuclear decoupling in rotating solids. J Chem Phys 103: 6951–6958

Bermel W, Bertini I, Felli IC, Piccioli M, Pierattelli R (2006) C-13-detected protonless NMR spectroscopy of proteins in solution. Prog Nucl Magn Reson Spectrosc 48:25–45

Bermel W, Bertini I, Felli IC, Matzapetakis M, Pierattelli R, Theil EC, Turano P (2007) A method for Cα direct-detection in protonless NMR. J Magn Reson 188:301–310

Bermel W, Felli IC, Kummerle R, Pierattelli R (2008) C-13 direct-detection biomolecular NMR. Concepts Magn Reson 32A:183–200

Bertini I, Luchinat C, Parigi G (2002) Paramagnetic constraints: an aid for quick solution structure determination of paramagnetic metalloproteins. Concepts Magn Reson 14:259–286

Cavanagh J, Fairbrother WJ, Palmer AG, Rance M, Skelton NJ (2007) Protein NMR spectroscopy. Academic Press, San Diego

Chandra K, Jaipuria G, Shet D, Atreya HS (2012) Efficient sequential assignments in proteins with reduced dimensionality 3D HN(CA)NH. J Biomol NMR 52:115–126

Chen L, Kaiser JM, Polenova T, Yang J, Rienstra CM, Müller LJ (2007a) Backbone assignments in solid-state proteins using J-based 3D Heteronuclear correlation spectroscopy. J Am Chem Soc 129:10650–10651

Chen L, Kaiser JM, Lai JF, Polenova T, Yang J, Rienstra CM, Müller LJ (2007b) J-based 2D homonuclear and heteronuclear correlation in solid-state proteins. Magn Reson Chem 45:S84–S92

Choy WY, Kay LE (2003) Model selection for the interpretation of protein side chain methyl dynamics. J Biomol NMR 25:325–333

Clore GM, Iwahara J (2009) Theory, practice, and applications of paramagnetic relaxation enhancement for the characterization of transient low-population states of biological macromolecules and their complexes. Chem Rev 109:4108–4139

Delaglio F, Grzesiek S, Vuister GW, Zhu G, Pfeifer J, Bax A (1995) NMRPIPE—a multidimensional spectral processing system based on unix pipes. J Biomol NMR 6:277–293

Elena B, Lesage A, Steuernagel S, Bockmann A, Emsley L (2005) Proton to carbon-13 INEPT in solid-state NMR spectroscopy. J Am Chem Soc 127:17296–17302

Gagne SM, Tsuda S, Spyracopoulos L, Kay LE, Sykes BD (1998) Backbone and methyl dynamics of the regulatory domain of troponin C: anisotropic rotational diffusion and contribution of conformational entropy to calcium affinity. J Mol Biol 278: 667–686

Gardner KH, Konrat R, Rosen MK, Kay LE (1996) An (H)C(CO)NH-TOCSY pulse scheme for sequential assignment of protonated methyl groups in otherwise deuterated N-15, C-13-labeled proteins. J Biomol NMR 8:351–356

Gardner KH, Rosen MK, Kay LE (1997) Global folds of highly deuterated, methyl-protonated proteins by multidimensional NMR. Biochemistry 36:1389–1401

Gross JD, Gelev VM, Wagner G (2003) A sensitive and robust method for obtaining intermolecular NOEs between side chains in large protein complexes. J Biomol NMR 25:235–242

Iwahara J, Tang C, Clore GM (2007) Practical aspects of (1)H transverse paramagnetic relaxation enhancement measurements on macromolecules. J Magn Reson 184:185–195

Jaipuria G, Thakur A, D'Silva P, Atreya HS (2010) High-resolution methyl edited GFT NMR experiments for protein resonance assignments and structure determination. J Biomol NMR 48:137–145

Jordan JB, Kovacs H, Wang Y, Mobli M, Luo R, Anklin C, Hoch JC, Kriwacki RW (2006) Three-dimensional ^{13}C-detected CH_3-TOCSY using selectively protonated proteins: facile methyl resonance assignment and protein structure determination. J Am Chem Soc 128:9119–9128

Kovacs H, Moskau D, Spraul M (2005) Cryogenically cooled probes—a leap in NMR technology. Prog Nucl Magn Reson Spectrosc 46:131–155

Metz G, Wu XL, Smith SO (1994) Ramped-amplitude cross polarization in magic-angle-spinning NMR. J Magn Reson, Series A 110:219–227

Metzler WJ, Wittekind M, Goldfarb V, Mueller L, Farmer BT (1996) Incorporation of H-1/C-13/N-15-{Ile, Leu, Val} into a perdeuterated, N-15-labeled protein: potential in structure determination of large proteins by NMR. J Am Chem Soc 118:6800–6801

Milardi D, Arnesano F, Grasso G, Magrì A, Tabbì G, Scintilla S, Natile G, Rizzarelli E (2007) Ubiquitin stability and the Lys 63-linked polyubiquitination site are compromised on copper binding. Angew Chem Int Ed 46:7993–7995

Nicholson LK, Kay LE, Baldisseri DM, Arango J, Young PE, Bax A, Torchia DA (1992) Dynamics of methyl-groups in proteins as studied by proton-detected C-13 NMR-spectroscopy—application to the leucine residues of staphylococcal nuclease. Biochemistry 31:5253–5263

Ottiger M, Delaglio F, Bax A (1998) Measurement of J and dipolar couplings from simplified two-dimensional NMR spectra. J Magn Reson 131:373–378

Rosen MK, Gardner KH, Willis RC, Parris WE, Pawson T, Kay LE (1996) Selective methyl group protonation of perdeuterated proteins. J Mol Biol 263:627–636

Swain M, Slomiany MG, Rosenzweig SA, Atreya HS (2010) High-yield bacterial expression and structural characterization of recombinant human insulin-like growth factor binding protein-2. Arch Biochem Biophys 501:195–200

Takegoshi K, Nakamura S, Terao T (2001) C-13-H-1 dipolar-assisted rotational resonance in magic-angle spinning NMR. Chem Phys Lett 344:631–637

Takegoshi K, Nakamura S, Terao T (2003) C-13-H-1 dipolar-driven C-13-C-13 recoupling without C-13 rf irradiation in nuclear magnetic resonance of rotating solids. J Chem Phys 118: 2325–2341

Thruber KR, Tycko R (2009) Measurement of sample temperature under magic angle spinning from the chemical shift and spin lattice relaxation rate of ^{79}Br in KBr powder. J Magn Reson 196:84–87

Tian Y, Chen LL, Niks D, Kaiser JM, Lai JF, Rienstra CM, Dunn MF, Mueller LJ (2009) J-Based 3D sidechain correlation in solid-state proteins. Phys Chem Chem Phys 11:7078–7086

Tugarinov V, Kay LE (2004) An isotope labeling strategy for methyl TROSY spectroscopy. J Biomol NMR 28:165–172

Tugarinov V, Hwang PM, Ollerenshaw JE, Kay LE (2003) Cross-correlated relaxation enhanced H-1-C-13 NMR spectroscopy of

methyl groups in very high molecular weight proteins and protein complexes. J Am Chem Soc 125:10420–10428

Tugarinov V, Hwang PM, Kay LE (2004) Nuclear magnetic resonance spectroscopy of high-molecular-weight proteins. Ann Rev Biochem 73:107–146

Tugarinov V, Choy WY, Orekhov VY, Kay LE (2005) Solution NMR-derived global fold of a monomeric 82-kDa enzyme. Proc Natl Acad Sci USA 102:622–627

Werbelow LG, Marshall AG (1973) Internal-rotation and nonexponential methyl nuclear relaxation for macromolecules. J Magn Reson 11:299–313

Zech SG, Olejniczak E, Hajduk P, Mack J, McDermott AE (2004) Characterization of protein—ligand interactions by high-resolution solid-state NMR spectroscopy. J Am Chem Soc 126: 13948–13953

Zheng DY, Huang YPJ, Moseley HNB, Xiao R, Aramini J, Swapna GVT, Montelione GT (2003) Automated protein fold determination using a minimal NMR constraint strategy. Protein Sci 12:1232–1246

Zhong L, Bamm VV, Ahmed MAM, Harauz G, Ladizhansky V (2007) Solid-state NMR spectroscopy of 18.5 kDa myelin basic protein reconstituted with lipid vesicles: spectroscopic characterisation and spectral assignments of solvent-exposed protein fragments. Biochim Biophys Acta Biomembranes 1768:3193–3205

Zwahlen C, Gardner KH, Sarma SP, Horita DA, Byrd RA, Kay LE (1998) An NMR experiment for measuring methyl–methyl NOEs in C-13-labeled proteins with high resolution. J Am Chem Soc 120:7617–7625